MOLSTR11501

Journal of Molecular Structure 000 (2000) 000–000

Journal of MOLECULAR STRUCTURE

www.elsevier.nl/locate/molstruc

A higher level ab initio quantum-mechanical study of the quadrupole moment tensor components of carbon dioxide ☆

R. Glaser*, Z. Wu, M. Lewis

Department of Chemistry, University of Missouri-Columbia, Columbia, MO 65211 USA

Received 22 December 1999; accepted 12 January 2000

Abstract

The quadrupolarity of carbon dioxide has been studied with higher level ab initio methods. Carbon dioxide exhibits {− + −} quadrupolarity in all directions and an explanation is provided of the origin of the sign of the diagonal elements Q_{ii}. The quadrupole moment tensor has been computed using restricted Hartree–Fock theory, second-order Møller–Plesset perturbation theory and quadratic configuration interaction theory. A variety of basis sets have been employed up to basis sets of the type [5s, 4p, 2d, 1f] (23s, 8p, 2d, 1f). The quadrupole moment tensor component $Q_{\parallel}$ of carbon dioxide falls in the range between −18.5 and −20.5 Debye Å. The quadrupole moment tensor components $Q_{\perp}$ of carbon dioxide are smaller, ranging from −14.5 to −15 Debye Å, and they are less sensitive to the choice of the theoretical model. The correlated methods consistently predict an increase of $Q_{\parallel}$ while they predict a more modest reduction of $Q_{\perp}$. It is for the opposing electron correlation effects on $Q_{\parallel}$ and $Q_{\perp}$ that the average values of the diagonal elements, $\langle Q_{ii} \rangle$, are essentially independent of the method and exhibit only a small variation depending on the basis set. On the other hand, the anisotropy of the quadrupolarity, the quadrupole moment Θ, is affected most by the opposing electron correlation effects on $Q_{\parallel}$ and $Q_{\perp}$. The accurate reproduction of the measured quadrupolarity $\Theta = -4.3$ Debye Å requires a theoretical model that employs both a good method and a good basis set. The results suggest that the use of second-order Møller–Plesset perturbation theory in conjunction with well-polarized triple-ζ basis sets provides a cost-effective and quite accurate method for the estimation of correlation effects on quadrupole moments.

Keywords: Quadrupole moment tensor components; Atomic charges; Anisotropy; Carbon dioxide; Electrostatic bonding; Ab initio calculations

1. Introduction

The most important reactions of heterocumulenes Y=C=X (X, Y = O, NH,…) involve nucleophilic attack across one of the C=X bonds. The nucleophilic addition of water to dicyclohexylcarbodiimide is widely used for dehydration [1–3]. We are particularly interested in the hydrolysis and acidolysis of carbodiimides because of their role as reactive intermediates in guanine deamination [4–12]. Over the past 40 years, carbodiimides have proliferated from reagents for peptide and nucleotide syntheses [13,14] to reagents in a wide array of chemical applications [15]. In spite of the widespread interest in carbodiimides, there have been surprisingly few mechanistic studies of their addition chemistry [16,17]. Computational studies were performed on the parent carbodiimide, HN=C=NH, and these focused on the geometry and spectroscopic properties

☆ Part 2 in the series "Nucleophilic additions to heterocumulenes."

* Corresponding author. Tel.: +1-573-882-0331; fax: +1-573-882-2754.

E-mail address: glaserr@missouri.edu (R. Glaser).

0022-2860/00/$ - see front matter
PII: S0022-2860(00)00658-X

of the equilibrium structure [18–20], on N-inversion [21,22] and on torsional-rotational dynamics [23]. The experimental characterization of carbodiimide is rather difficult and the structure [24], vibrational properties [25,26] and the dipole moment [27] have been determined only recently. Very little is known about nucleophilic additions to carbodiimides in general and about the hydrolysis in particular [28]. The hydrolysis of the closely related and isoelectronic carbon dioxide, on the other hand, has been studied in much more detail. The enzymatically catalyzed [29,30] and the non-enzymatically catalyzed reactions were studied [31–33] and the latter reaction also received considerable attention from theoreticians [34–39].

In the first step of nucleophilic addition, heterocumulenes form rather strong van-der-Waals complexes with nucleophiles. The bonding in these complexes is largely electrostatic with contributions due to hydrogen-bonding, other dipole–dipole interactions as well as dipole–quadrupole interactions. To understand better the electrostatic bonding in these complexes, one needs to learn about the charge distribution and the electrostatic moments of the heterocumulenes. The quadrupole moment and the electrical dipole polarizability are two pertinent properties in this context and neither of these quantities has been measured for carbodiimide. Both of these quantities are "difficult" to compute, that is, these properties are known to be sensitive to the choice of theoretical level. Hence, the establishment of the accuracy of a given theoretical level for the computation of these properties becomes a key issue in the quality assessment of studies of electrostatic bonding. The purely theoretical approach would entail the gradual improvement in the theoretical level until all properties have converged toward their respective asymptotic values. This approach, while rigorous, remains impractical even for molecules of modest size. A more practical approach relies on the establishment of the accuracy of a given theoretical level for a closely related system for which experimental data are available. In the present study, we present the results of a higher level ab initio quantum-mechanical study of the bond polarity and of the quadrupole moment tensors of carbon dioxide. The experimental data available for carbon dioxide are employed to establish the accuracies of a great variety of hierarchically ordered theoretical levels for the computation of these properties. The knowledge of these theoretical level dependencies then may guide the choice of the theoretical levels in our studies of the hydrolysis of carbon dioxide [40] and of carbodiimide [28].

2. Theoretical methods and computations

2.1. Atomic charges and quadrupole moment tensor components

The natural population analysis (NPA) [41,42] was employed to characterize the intramolecular charge transfer. The Pauling electronegativities of C and O are 2.55 and 3.44, respectively [43].

The elements Q_{ij} of the quadrupole moment tensor are defined as

$$Q_{ij} = \int \sigma(\mathbf{r}) r_i r_j \, \mathrm{d}\mathbf{r} \qquad (i = x, y, z)$$

where $\sigma(\mathbf{r})$ is the charge density distribution and r_i and r_j are the components of the distance vector (x, y, z) from the molecular center. Alternatively, one might separate the terms that are caused by the n nuclei with their nuclear charges $Z(n)$ and the electron density distribution $\rho(\mathbf{r})$ and the expression for the tensor elements becomes

$$Q_{ij} = \sum Z(n) r_i(n) r_j(n) - \int |\rho(\mathbf{r})| r_i r_j \, \mathrm{d}\mathbf{r}$$

and for the diagonal elements this equation reduces to the form

$$Q_{ij} = \sum Z(n) r_i(n)^2 - \int |\rho(\mathbf{r})| r_i^2 \, \mathrm{d}\mathbf{r}.$$

The off-diagonal tensor elements Q_{ij} vanish whenever the molecule has a plane of symmetry perpendicular to either one of the coordinates i or j. Carbon dioxide always was placed on the x-axis with carbon at the origin. The C_2-z-axis transforms (x, y, z) into ($-x$, $-y$, z) and integrals containing $r_i r_j$ will vanish whenever the symmetry operation leads to an odd number of sign changes. The off-diagonal elements Q_{xz} and Q_{yz} thus vanish for carbon dioxide. The third off-diagonal element Q_{yz} also vanishes due to the C_2-y-axis. In the chosen orientation, the diagonal element Q_{xx} characterizes the electron density distribution along the C=O bonds and the diagonal elements Q_{yy}

Table 1
Description of basis sets

Basis set	5d or 6d and 7f or 10f	Basis functions C, O	Primitive functions C, O
6-31G*	6d	[3s, 2p, 1d]	(10s, 4p, 1d)
6-311G*	5d	[4s, 3p, 1d]	(11s, 5p, 1d)
6-311 + G*	5d	[5s, 4p, 1d]	(12s, 6p, 1d)
6-311G(2d,p)	5d	[4s, 3p, 2d]	(11s, 5p, 2d)
6-311 + G(2d)	5d	[5s, 4p, 2d]	(12s, 6p, 2d)
6-311G(2df)	5d, 7f	[4s, 3p, 2d, 1f]	(11s, 5p, 2d, 1f)
6-311 + G(2df)	5d, 7f	[5s, 4p, 2d, 1f]	(12s, 6p, 2d, 1f)
D95V(d)	6d	[3s, 2p, 1d]	(10s, 5p, 1d)
D95V + (d)	6d	[4s, 3p, 1d]	(11s, 6p, 1d)
cc-pVDZ	5d	[3s, 2p, 1d]	(19s, 5p, 1d)
cc-pVDZ +	5d	[4s, 3p, 1d]	(20s, 6p, 1d)
cc-pVTZ	5d, 7f	[4s, 3p, 2d, 1f]	(22s, 7p, 2d, 1f)
cc-pVTZ +	5d, 7f	[5s, 4p, 2d, 1f]	(23s, 8p, 2d, 1f)

and $_{Q_{zz}}$ are equal and characterize the π-systems. For carbon dioxide, the "quadrupole moment" Θ is known from measurements (vide infra). Such measured quadrupole moments have the quality of a "quadrupole moment tensor anisotropy" since the unique quadrupole moment Θ is related to the quadrupole moment tensor components by way the equation

$$\Theta = Q_{\parallel} - Q_{\perp}$$

and with the orientation selected one obtains

$$\Theta = Q_{yy} - Q_{xx}$$

We will also discuss the average of the diagonal quadrupole moment tensor elements $\langle Q_{ii} \rangle$ which is defined by

$$\langle Q_{ii} \rangle = (Q_{xx} + Q_{yy} + Q_{zz})/3.$$

Molecular quadrupole moments are on the order of 10^{-26} e.s.u. A list of conversion factors for various units employed for electrostatic moments can be found in a recent review [44]. Some of the more commonly used units are related as follows: 1 e.s.u. $= 3.33564 \times 10^{-14}$ C m^2 and 1 C m^2 $= 2.99792 \times 10^{39}$ Debye Å. We will be reporting quadrupole moments in units of Debye Å.

2.2. Description of ab initio theoretical levels

The determination of the desired properties requires the electron density distribution $\rho(\mathbf{r})$ for a given nuclear configuration. We have determined electron density functions $\rho(\mathbf{r})$ using several theoretical methods [45,46]. Restricted Hartree–Fock (RHF) theory is the obvious starting point. RHF theory includes only a part of the electron correlation between same spin electrons and post-HF methods need to be employed to more fully account for electron correlation. We have employed both Møller–Plesset perturbation theory and quadratic configuration interaction theory to that effect. Both of these methods are size-consistent. All single and double excitations were included in the perturbation calculations and the active space of these second-order Møller–Plesset calculations included all electrons and all molecular orbitals, MP2(full). The quadratic CI theory [47,48] is the most sophisticated theory applied here. In this advanced method, the RHF reference wavefunction is used as the starting point of a variational configuration interaction calculation that includes single and double excitations, QCISD. The active space included all valence electrons and the entire virtual space while the three core molecular orbitals were kept frozen.

Several basis sets were employed in conjunction with these three methods (Table 1). The smallest of these basis sets was the 6-31G* basis set [49–51]. Split-valence basis sets are required to allow for anisotropies at the atoms and these are especially important in computations of quadrupole moment tensor elements. The inclusion of polarization functions in the basis sets of the C- and O- is mandatory to

Table 2
Energies, bond length and atomic charge of carbon dioxide (total energies in atomic units, bond lengths in Å and charges in atomic units)

Theoretical level	Energy	d(CO)	NPA(C)
RHF-theory			
6-31G*	−187.634176	1.143	1.243
6-31+G*	−187.638787	1.143	1.233
6-311G*	−187.687590	1.135	1.200
6-311+G*	−187.691561	1.136	1.194
6-311G(2d)	−187.693795	1.135	1.219
6-311+G(2d)	−187.697518	1.136	1.215
6-311G(2df)	−187.702502	1.135	1.225
6-311+G(2df)	−187.706001	1.135	1.219
D95V(d)	−187.676118	1.145	1.265
D95V+(d)	−187.679203	1.144	1.261
cc-pVDZ	−187.652896	1.141	1.280
cc-pVDZ+	−187.711012	1.140	1.280
cc-pVTZ	−187.709909	1.136	1.188
cc-pVTZ+	−187.711012	1.136	1.187
MP2(full)-theory			
6-31G*	−188.118363	1.179	0.960
6-31+G*	−188.129361	1.180	0.955
6-311G*	−188.255330	1.168	0.935
6-311+G*	−188.263140	1.169	0.930
6-311G(2d)	−188.300135	1.167	0.960
6-311+G(2d)	−188.307493	1.168	0.956
6-311G(2df)	−188.358401	1.165	0.964
6-311+G(2df,p)	−188.364973	1.165	0.959
D95V(d,p)	−188.152082	1.181	1.003
D95V++(d,p)	−188.161273	1.181	0.990
cc-pVDZ	−188.140206	1.177	0.999
cc-pVDZ+	−188.140205	1.176	0.901
cc-pVTZ	−188.348864	1.166	0.919
cc-pVDZ+	−188.360203	1.166	0.913
QCISD(fc)-theory			
6-31G*	−188.106376	1.173	1.028
6-31+G*	−188.115836	1.174	1.023
6-311G*	−188.195034	1.162	0.998
6-311+G*	−188.201858	1.163	0.993
6-311G(2d)	−188.232324	1.161	1.024
6-311+G(2d)	−188.238663	1.162	1.021
6-311G(2df)	−188.289576	1.159	1.030
6-311+G(2df)	−188.295050	1.159	1.026
D95V(d,p)	−188.141910	1.176	1.065
D95V+(d)	−188.149916	1.175	1.055
cc-pVDZ	−188.132960	1.170	1.063
cc-pVDZ+	−188.150994	1.170	0.967
cc-pVTZ	−188.301798	1.161	0.989
cc-pVTZ+	−188.306096	1.161	0.984
Experimental value[a]		1.162	

[a] From Ref. [44].

account for the reduced symmetry of the atomic orbitals in the molecules. The next two basis sets employed are 6-311G** and 6-311++G** [52–54]. The step from a double-ζ to a triple-ζ valence description is a major improvement. The addition of the diffuse functions produces a quadruple-ζ type basis set and might further refine the electron density distribution especially with a view to the π-density and the lone pairs. The larger basis sets are especially advantageous in that they provide improved virtual spaces in the correlation treatments. One can further improve on these basis sets by improvement of the number and the type of the polarization functions and we have considered two options [55]. At the 6-311G(2d) level, two sets of d-functions are used and a linear optimization of the d-orbital exponent is accomplished in this way. At the next stage, a set of f-functions is added on top of the two sets of d-orbitals, 6-311G(2df). Finally, both of these basis sets are augmented with diffuse functions and the resulting basis sets 6-311 + G(2d) and 6-311 + G(2df), respectively, are the largest Pople basis sets employed in the present study.

The valence double-ζ basis set D95V(d) also was employed [56]. This basis set offers a slight advantage in comparison to the 6-31G* basis set in that it does not use the same primitive exponents for s- and p-orbitals and that it uses one more primitives for the expansion of the p-basis functions on the heavy atoms. We have also considered some of Dunning's correlation-consistent basis sets cc-pVnZ [57]. In terms of the number of basis functions, this cc-pVDZ basis set is comparable to the 6-31G* basis sets of first-row atoms. In terms of primitives, however, the cc-pVDZ is much larger and this is especially so for the number of s-primitives. The cc-pVTZ basis sets is comparable to the 6-311G(2df,p) basis set in terms of basis functions but, again, the former features a much larger number of primitives. The final refinement of these three basis sets again consisted in the augmentation by diffuse functions and the resulting basis sets are denoted D95V++(d,p), cc-pVDZ++ and cc-pVTZ++, respectively. These diffuse function augmentations employed single sp-shells on first row-atoms and the exponents are those used in the Pople basis sets. Note that this procedure differs from the usual diffuse function augmentation of the cc-pVnZ type basis sets which adds one diffuse

Table 3
Quadrupole moments of carbon dioxide (all values in Debye Å)

Theoretical level	Q_{xx}	$Q_{yy} = Q_{zz}$	$\langle Q \rangle$	Q
RHF-theory				
6-31G*	−19.915	−14.456	−16.275	−5.459
6-31+G*	−20.335	−14.723	−16.594	−5.612
6-311G*	−19.995	−14.441	−16.292	−5.554
6-311+G*	−20.249	−14.648	−16.515	−5.601
6-311G(2d)	−19.457	−14.519	−16.165	−4.938
6-311+G(2d)	−19.705	−14.727	−16.386	−4.979
6-311G(2df)	−19.589	−14.499	−16.196	−5.090
6-311+G(2df)	−19.797	−14.693	−16.395	−5.103
D95V(d)	−19.949	−14.594	−16.379	−5.355
D95V+(d)	−20.155	−14.695	−16.515	−5.461
cc-pVDZ	−19.678	−14.415	−16.170	−5.263
cc-pVDZ+	−19.648	−14.513	−16.668	−5.134
cc-pVTZ	−19.663	−14.551	−16.255	−5.112
cc-pVTZ+	−19.664	−14.585	−16.278	−5.079
MP2(full)-theory				
6-31G*	−19.039	−14.723	−16.162	−4.316
6-31+G*	−19.734	−15.153	−16.668	−4.599
6-311G*	−19.131	−14.698	−16.175	−4.433
6-311+G*	−19.592	−15.003	−16.533	−4.589
6-311G(2d)	−18.763	−14.779	−16.107	−3.985
6-311+G(2d)	−19.187	−15.075	−16.445	−4.112
6-311G(2df)	−18.799	−14.726	−16.084	−4.073
6-311+G(2df,p)	−19.170	−15.002	−16.391	−4.169
D95V(d,p)	−19.202	−14.959	−16.373	−4.243
D95V++(d,p)	−19.545	−15.128	−16.600	−4.417
cc-pVDZ	−18.794	−14.701	−16.065	−4.092
cc-pVDZ+	−18.921	−14.850	−16.207	−4.071
cc-pVTZ	−18.921	−14.811	−16.181	−4.110
cc-pVDZ+	−18.940	−14.869	−16.226	−4.071
QCISD(fc)-theory				
6-31G*	−19.357	−14.669	−16.232	−4.688
6-31+G*	−19.995	−15.043	−16.693	−4.952
6-311G*	−19.406	−14.632	−16.224	−4.774
6-311+G*	−19.822	−14.909	−16.546	−4.913
6-311G(2d)	−18.991	−14.717	−16.142	−4.274
6-311+G(2d)	−19.368	−14.984	−16.445	−4.384
6-311G(2df)	−19.039	−14.660	−16.120	−4.379
6-311+G(2df)	−19.358	−14.903	−16.388	−4.455
D95V(d,p)	−19.505	−14.890	−16.428	−4.615
D95V+(d)	−19.811	−15.037	−16.628	−4.774
cc-pVDZ	−19.089	−14.642	−16.124	−4.447
cc-pVDZ+	−19.173	−14.771	−16.238	−4.402
cc-pVTZ	−19.140	−14.735	−16.203	−4.405
cc-pVTZ+	−19.146	−14.778	−16.234	−4.368
Experimental values[a]				−4.278

[a] From Refs. [45,46], see text.

Table 4
Vibrational frequencies of carbon dioxide (all values in cm^{-1})

Theoretical level	ν_{π}	$\nu_{sym.}$	$\nu_{asym.}$
RHF/6-31G*	642	1336	2454
RHF/6-311G*	661	1344	2461
RHF/6-311 + G*	661	1338	2438
MP2(full)/6-31G*	642	1336	2454
MP2(full)/6-311G*	661	1344	2461
MP2(full)/6-311 + G*	661	1338	2438
QCISD/6-31G*	652	1364	2417
QCISD/6-311G**	675	1374	2431
QCISD/6-311 + G*	672	1369	2410
Experimental values[a]	667.40	1388.17	2349.16

[a] From Ref. [44].

function of each function type (including d- and f-functions).

We have optimized the structure of carbon dioxide with each of the three theoretical methods and with each of the basis sets.

The ab initio calculations were carried out with the program GAUSSIAN 94 [58] on a Silicon Graphics PowerChallenge L minisupercomputer. Total energies, optimized bond lengths and atomic charges are documented in Table 2. Quadrupole monent tensor components are summarized in Table 3. Vibrational frequencies are summarized in Table 4.

3. Results and discussion

3.1. Experimental data for carbon dioxide

The values for the experimental bond length (Table 2) and the measured vibrational frequencies (Table 4) of carbon dioxide were taken from the compilation by Herzberg [59].

The electrical quadrupole moment Θ of gaseous CO_2 was determined three times by measurement of the linear birefringence in an electric field gradient [60,61]. The original measurement yielded a value of $\Theta = -14.34 \pm 0.7 \times 10^{-40}$ C m^2 ($-4.3 \pm 0.2 \times 10^{-26}$ e.s.u.) and this value was subsequently refined to $\Theta = -14.27 \pm 0.61 \times 10^{-40}$ C m^2. The computed quadrupole moment and its components are given in units of Debye Å and the best experimental value is 4.278 Debye Å (Table 3).

3.2. Computed bond lengths and atomic charges

The CO bond lengths and the atomic charges show clear-cut theoretical level dependencies. The

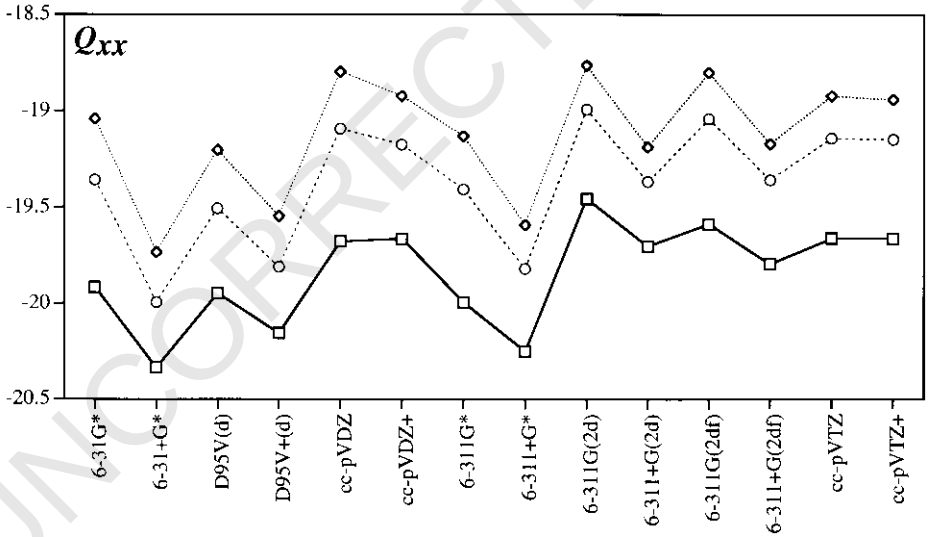

Fig. 1. Theoretical level dependency of the quadrupole tensor component $Q_{xx} = Q_{\|}$ of carbon dioxide. RHF data are marked by squares and connected by solid lines, MP2 data are marked by diamonds and connected by dotted lines, and QCISD data are marked by circles and connected by dashed lines.

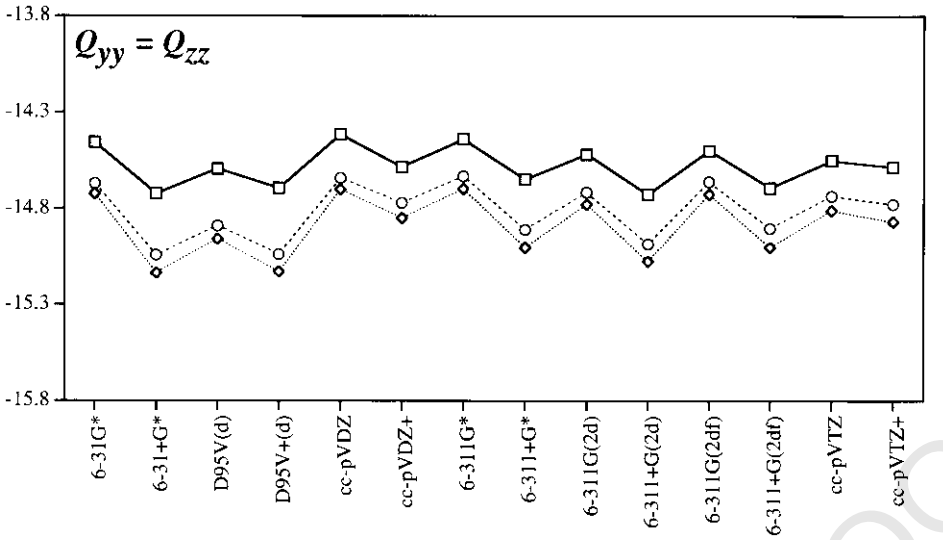

Fig. 2. Theoretical level dependency of the quadrupole tensor component $Q_{yy} = Q_{zz} = Q_{\perp}$ of carbon dioxide. Symbols refer to the same methods as in Fig. 1 As with Fig. 1, this graph is drawn with an ordinate window of 2 Debye Å.

theoretical model dependencies are correlated and, hence, we discuss structures and atomic charges together. In general, RHF theory overestimates bond polarity. With the lack of reducing electron–electron repulsion, RHF has no choice but to seek optimal intramolecular electrostatic stabilization with the result of the higher bond polarities and concomitantly underestimated bond lengths.

The CO bond length is systematically underestimated at the RHF level with deviations between −0.017 and −0.026 Å. Note that the largest deviations occur with the better basis sets. At the MP2

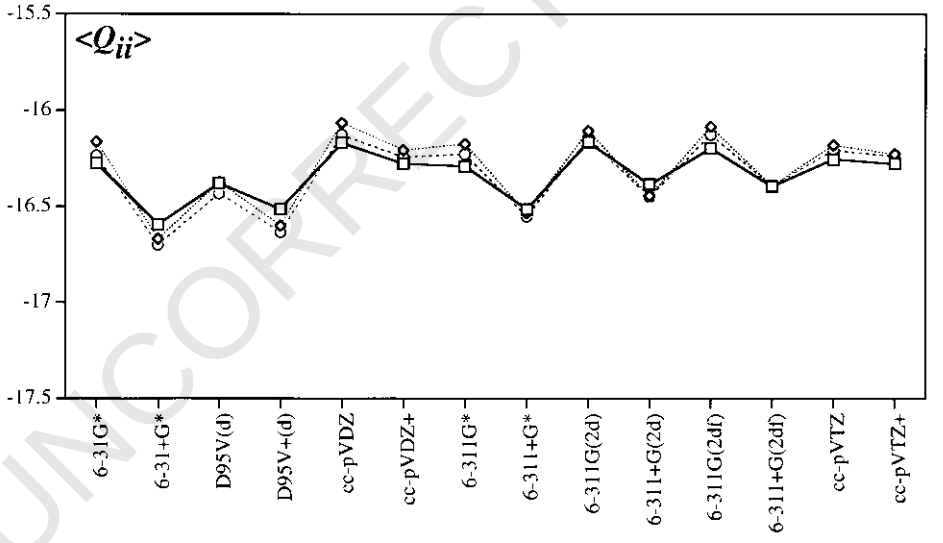

Fig. 3. Theoretical level dependency of the average $\langle Q \rangle$ of the diagonal elements of the quadrupole tensor components of carbon dioxide. Symbols refer to the same methods as in Figs. 1 and 2. As with Figs. 1 and 2, this graph is drawn with an ordinate window of 2 Debye Å.

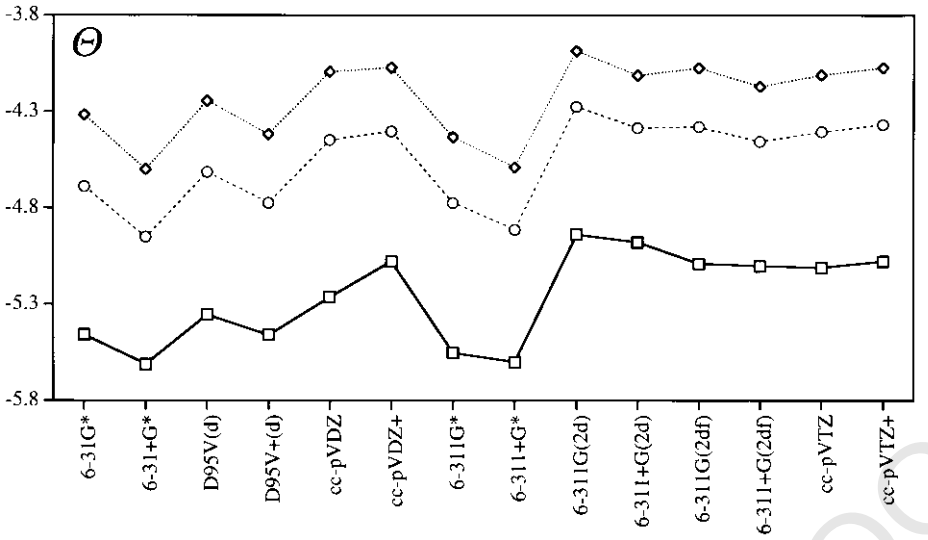

Fig. 4. Theoretical level dependency of the quadrupole moment Θ of carbon dioxide. Symbols refer to the same methods as in Figs. 1–3. The graph is drawn with the same vertical scale as are the graphs in Figs. 1–3, an ordinate window of 2 Debye Å.

and QCISD levels, the computed bond lengths scatter about the experimental value and the deviations are less than 0.01 Å at all levels employing triple-ζ basis sets or better. At these levels, the computed structures have converged to the experimental value. The natural charges computed with the RHF wave functions for carbon range from 1.19 to 1.28. At the correlated levels, the carbon charge is significantly diminished, it ranges from 0.96 to 1.03, and basis set dependencies are relatively minor and certainly less than the dependency on the method.

3.3. The quadrupolarity of carbon dioxide

The non-zero quadrupole moment tensor components of carbon dioxide are given in Table 3. The theoretical level dependencies are better revealed by graphical analysis of trends. In Figs. 1–3, variations of the quadrupole moment tensor components $Q_{xx} = Q_{\|}$, of $Q_{yy} = Q_{zz} = Q_{\perp}$ and of the average $\langle Q_{ii} \rangle$ of the diagonal elements are shown, respectively. Fig. 4 shows the computed quadrupole moments Θ of carbon dioxide providing anisotropy information on the quadrupolarity. In all of these figures, we have ordered the data with increasing quality of the basis set from left to right. While this ordering is not rigorous, the ordering selected is reasonable. Double-ζ basis sets are located on the left and triple-ζ basis sets are located on the right. Note that the diffuse-function augmented basis set always follows immediately to the right of the same basis set but without that augmentation. Hence, a diffuse-function augmented double-ζ basis set formally is of a triple-ζ quality but we list it still with the double-ζ basis sets. Within the two main blocs, the basis sets are ordered in a way that reflects more flexibility in the basis functions (e.g. V95D vs. 6-31G*) or more primitives (e.g. cc-VDZ vs. 6-31G* or V95D), or more sets of polarization functions, and more types of polarization functions.

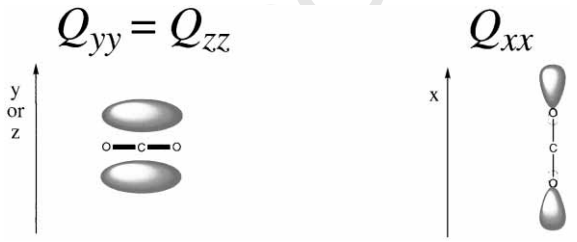

Scheme 1.

All of the diagonal elements of the quadrupole moment tensor of carbon dioxide are negative. Negative Q_{ii} values indicate that, on r^2-weighted average, the negative charge distribution is farther removed

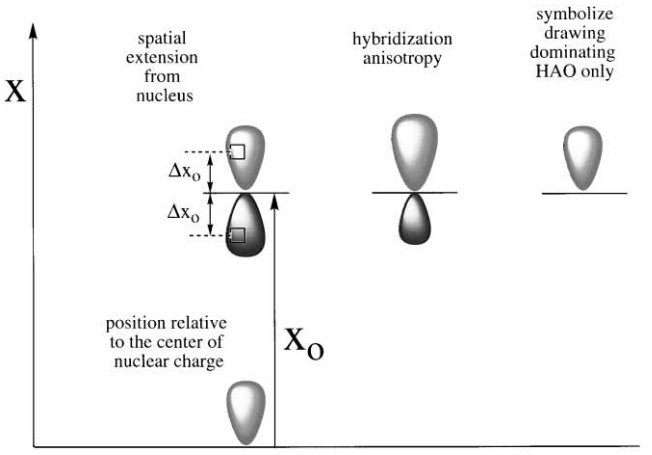

Scheme 2.

from the molecular center of the nuclear charges. Hence, in all three independent directions carbon dioxide is characterized by the quadrupolarity $\{- + -\}$.

The drawings in Scheme 1 may serve to illustrate graphically the origins of the diagonal quadrupole tensor moments of carbon dioxide. The negative sign of $Q_{yy} = Q_{zz} = Q_{\perp}$ is easily understood. Moving through a π-system perpendicular to the molecular axis one first encounters the negative region of the π-cloud, then the positive area of the nuclei, and then the second negative region of the π-cloud. The $\{- + -\}$ quadrupolarity $Q_{\perp}$ is thus intuitively easy to grasp and $Q_{\perp} < 0$ has to result since the nuclei do not contribute to $Q_{\perp}$ at all. It is important to realize that $Q_{\perp}$ is not only a function of the π-molecular orbitals but also contains contributions from the σ-molecular orbitals. The latter are neglected in the drawings in Scheme 1, but the contributions of the σ-molecular orbitals to $Q_{\perp}$ actually are quite sizeable.

To rationalize the quadrupole moment tensor components Q_{xx} is more involved. The polarity of the C–O bond of carbon dioxide is high and the O-atoms are the negative poles. It is important to realize that these features do not guarantee a negative quadrupole moment tensor component Q_{xx}, and, hence, they also do not explain the sign of Q_{xx}. Which feature of the electron density distribution of carbon dioxide is it, then, that causes the negative quadrupole moment tensor element Q_{xx}? Consider the electron density distributions associated with two degenerate sp_x hybrid orbitals centered at a distance x_0 from the molecular center of nuclear charge. The positions $x_0 + \Delta_x$ and $x_0 - \Delta_x$ are equidistant from the position x_0. The volume elements of electron density at the positions $x_0 - \Delta_x$ and $x_0 + \Delta_x$, respectively, contribute $-|\rho(\mathbf{r})| \times (x_0 - \Delta x)^2$ and $-|\rho(\mathbf{r})| \times (x_0 + \Delta x)^2$, and the combined contribution of these two volume elements to Q_{xx} is $-|\rho(\mathbf{r})| \times (2x_0^2 + 2\Delta x^2)$. An atom-centered electron density component that is symmetrical with regard to that atom contributes to Q_{xx} and the contribution increases (i) with the distance of the atom from the center of nuclear charge and (ii) with the spatial extension of the orbital (influences how large Δx can become). This is illustrated in Scheme 2. At the next level of sophistication one might consider differences in the shapes of the approximate sp hybrid orbitals. One of the hybrid orbitals might be more spatially extended and this "hybridization anisotropy" is illustrated to the right in Scheme 2. Note that the electron density around the O-atom will contribute a negative amount to Q_{xx} even if the electron density around that atom is not polarized in the x-direction. In reality, the electron density at the O-atoms does show a polarization in the x-direction to place more electron density behind the O-atom and this hybridization anisotropy will increase Q_{xx}. The O-sp-type hybrid orbital of the O lone pair is spatially more extended than the respective O-sp-type hybrid orbital of the C–O bond. This statement makes physical sense because the electrons involved in CO bonding are more contracted due to the higher attraction term in the

one-electron core Hamiltonian of the CO bonding MO. Extended basis sets are required to adequately describe this O-atom anisotropy because the greater spatial extension of the O-density in the lone pair region requires the use of greater contribution of the outer C-p-basis function(s). As to the C-atom, its contribution to Q_{xx} will be negative as well. The C-nucleus does not contribute at all and the electron density associated with the sp_x orbitals gives rise to a negative contribution to Q_{xx} (even though the C-atom is positively charged.) The Q_{xx} value of carbon dioxide is dominated by the contributions by the O-atoms, simply because $\langle X_0 \rangle$ is large for the O-atoms while $\langle X_0 \rangle = 0$ for the C-atom.

The quadrupolarity Q_{xx} can therefore be understood as the result of three effects: (i) atom positioning, x_0; (ii) hybrid orbital spatial extension, Δx; and (iii) hybridization anisotropy. These insights suggest a simple graphical notation for the discussion of the origin of quadrupole moments. For all atom-centered sets of C-sp-type hybrid orbital, we draw only the one(s) that is (are) oriented away from the center of nuclear charge and its (their) direction will indicate this atom's contribution to the electronic quadrupole moment component. For carbon dioxide, this leaves only the O-lone pairs since the contributions from the C-atom remains small ($\langle X_0 \rangle = 0$).

The quadrupole moment tensor component $Q_{xx} = Q_{\parallel}$ of carbon dioxide falls in the range between -18.5 and -20.5 Debye Å. The theoretical model dependency is quite pronounced (Fig. 1) but all values are within 2 Debye Å and the relative change is less than 10% and much better in most cases. The quadrupole moment tensor components $Q_{yy} = Q_{zz} = Q_{\perp}$ of carbon dioxide are smaller, they range from -14.5 to -15 Debye Å, and they vary less depending on the theoretical model (Fig. 2); all values are within 1 Debye Å and the relative change is less than 7%. The addition of diffuse basis function to the basis set consistently lowers $Q_{\perp}$ and the magnitude of the change can be as high as 0.5 Debye Å. A similar trend also occurs for $Q_{\parallel}$ (except for the cc-VDZ and cc-VTZ cases). The correlated methods consistently predict an increase of $Q_{\parallel}$ and a more modest reduction of $Q_{\perp}$.

It is for the opposing electron correlation effects on $Q_{\parallel}$ and $Q_{\perp}$ that the average values of the diagonal elements, $\langle Q_{ii} \rangle$ are essentially independent of the method and exhibit only a small variation depending on basis set (Fig. 3). On the other hand, it is now also clear why the anisotropy of the quadrupolarity, the quadrupole moment Θ, is affected most by the correlation effects (Fig. 4). The correlated methods predict Θ values that are about 1 Debye Å less negative than the values computed at the RHF level.

Only the quadrupolarity Θ is experimentally observable and its measured value is -4.3 Debye Å. This value is reproduced very well at all levels of QCISD theory with basis sets better than 6-311G(2d) (Fig. 4). The theoretical level QCISD/6-311G(2d) is a rather sophisticated level and for many important chemical problems, the use of this theoretical level is not practical. With a view to studies of larger systems, Fig. 4 is rather significant. This figure shows that the basis set dependency is about the same irrespective of the method and that the method dependency is about the same independent of basis set. Hence, one must use both a good method and a good basis set. But just how good is good? Fig. 4 shows that the use of second-order Møller–Plesset perturbation theory in conjunction with well-polarized triple-ζ basis sets provides a cost-effective and quite accurate method for the estimation of correlation effects on quadrupole moments.

Acknowledgements

This research was supported by the MU Research Council. M.L. thanks the Natural Sciences and Engineering Research Council (NSERC) of Canada for a post-graduate scholarship type B.

References

[1] T. Schimzu, N. Seki, H. Taka, N. Kamigata, J. Org. Chem. 61 (1996) 6013.
[2] E. Schuster, C. Hesse, D. Schumann, Synlett 12 (1991) 916.
[3] G.A. Olah, A. Wu, O. Farooq, Synthesis 7 (1989) 568.
[4] J.L. Caulfield, J.S. Wishnok, S.R. Tannenbaum, J. Biol. Chem. 273 (1998) 12 689.
[5] C.J. Burrows, J.G. Muller, Chem. Rev. 98 (1998) 1109.
[6] R. Glaser, M.-S. Son, J. Am. Chem. Soc. 118 (1996) 10 942.
[7] R. Glaser, S. Rayat, M. Lewis, M.-S. Son, S. Meyer, J. Am. Chem. Soc. 121 (1999) 6108.
[8] R. Glaser, M. Lewis, Org. Lett. 1 (1999) 273.
[9] T. Suzuki, R. Yamaoka, M. Nishi, H. Ide, K. Makino, J. Am. Chem. Soc. 118 (1996) 2515.
[10] T. Suzuki, K. Kanaori, K. Tajima, K. Makino, Nucleic Acids Symp. Ser. 37 (1997) 313.

[11] T. Suzuki, M. Yamada, K. Kanaori, K. Tajima, K. Makino, Nucleic Acids Symp. Ser. 39 (1998) 177.
[12] L.T. Lucas, D. Gatehouse, D.E.G. Shuker, J. Biol. Chem. 274 (1999) 18 319.
[13] H.G. Khorana, Chem Rev. 53 (1953) 145.
[14] F. Kurzer, K. Douraghi-Zadeh, Chem. Rev. 67 (1967) 107.
[15] A. Williams, I.T. Ibrahim, Chem. Rev. 81 (1981) 589.
[16] M. Slebioda, Tetrahedron 51 (1995) 7829.
[17] I.T. Ibrahim, A. Williams, J. Chem. Soc. Perkin Trans. II (1982) 1459.
[18] M.T. Nguyen, N.V. Riggs, L. Radom, M. Winnewisser, B.P. Winnewisser, M. Birk, Chem. Phys. 122 (1988) 305.
[19] J. Bertran, A. Oliva, J. Jose, M. Duran, P. Molina, M. Alajarin, C.L. Leonardo, Elguero, J. Chem. Soc. Perkin Trans. 2 (1992) 299.
[20] J. Koput, W. Jabs, M. Winnewisser, Chem. Phys. Lett. 295 (1998) 462.
[21] M.T. Nguyen, T.-K.J. Ha, Chem. Soc. Perkin Trans. II (1983) 1297.
[22] J.M. Lehn, B. Munsch, Theor. Chim. Acta 12 (1968) 91.
[23] P. Pracna, M. Winnewisser, B.P. Winnewisser, J. Mol. Spectrosc. 162 (1993) 127.
[24] W. Jabs, M. Winnewisser, S.P. Belov, F. Lewen, F. Maiwald, G. Winnewisser, Mol. Phys. 97 (1999) 213.
[25] S.T. King, J.H. Strope, J. Chem. Phys. 54 (1971) 1289.
[26] A. Daoudi, C. Pouchan, H. Sauvaitre, J. Mol. Struct. 89 (1982) 103.
[27] M. Birk, M. Winnewisser, E.A. Cohen, J. Mol. Spectrosc. 136 (1989) 402.
[28] M. Lewis, R. Glaser, J. Am. Chem. Soc. 120 (1998) 8541.
[29] K.M. Merz, L. Banci, J. Am. Chem. Soc. 119 (1997) 863.
[30] D.W. Christianson, C.A. Fierke, Acc. Chem. Res. 29 (1996) 331.
[31] J.K. Terlouw, C.B. Lebrilla, J. Schwarz, Angew. Chem. Int. Ed. Engl. 26 (1987) 354.
[32] J.F. Marlier, M.H. O'Leary, J. Am. Chem. Soc. 106 (1984) 5054.
[33] E. Magid, B.O. Turbeck, Biochim. Biophys. Acta 165 (1968) 515.
[34] M.T. Nguyen, G. Raspoet, L.G. Vanquickenborne, P.T. Van Duijnen, J. Phys. Chem. A 101 (1997) 7379.
[35] K.M. Merz, J. Am. Chem. Soc. 112 (1990) 7973.
[36] J.-Y. Liang, W.N. Lipscomb, J. Am. Chem. Soc. 108 (1986) 5051.
[37] M.T. Nguyen, T.-K. Ha, J. Am. Chem. Soc. 106 (1984) 599.
[38] B. Jonsson, G. Karlstrom, H. Wennerstrom, S. Forsen, B. Roos, J. Almlof, J. Am. Chem. Soc. 99 (1977) 4628.
[39] L. Radom, W.A. Lathan, W.J. Hehre, J.A. Pople, Aust. J. Chem. 25 (1972) 1601.
[40] M. Lewis, R. Glaser, submitted for publication.
[41] E.D. Glendening, A.E. Reed, J.E. Carpenter, F. Weinhold, NBO Version 3.1.
[42] E.D. Glendening, F. Weinhold, J. Comput. Chem. 19 (1998) 628 (and references cited therein).
[43] WebElements—The Periodic Table on the Web. http://www.webelements.com/ (accessed, November 30, 1999).
[44] M.A. Spackman, Chem. Rev. 92 (1992) 1769.
[45] A. Szabo, N.S. Ostlund, Modern Quantum Chemistry: Introduction to Advanced Electronic Structure Theory, MacMillan, New York, 1982.
[46] W.L. Hehre, L. Radom, P.V.R. Schleyer, J.A. Pople, Ab Initio Molecular Orbital Theory, Wiley, New York, 1986.
[47] M. Head-Gordon, J.A. Pople, K. Raghavachari, J. Chem. Phys. 87 (1987) 5968.
[48] C. Hampel, K.A. Peterson, H.-J. Werner, Chem. Phys. Lett. 120 (1992) 1.
[49] W.J. Hehre, R. Ditchfield, J.A. Pople, J. Chem. Phys. 56 (1972) 2257 (6-31G*).
[50] M.M. Francl, W.J. Petro, W.J. Hehre, J.S. Binkley, M.S. Gordon, D.J. DeFrees, J.A. Pople, J. Chem. Phys. 77 (1982) 3654 (6-31G*).
[51] P.C. Hariharan, J.A. Pople, Theor. Chim. Acta 28 (1973) 213.
[52] R. Krishnan, J.S. Binkley, R. Seeger, J.A. Pople, J. Chem. Phys. 72 (1980) 650 (6-311G**).
[53] A.D. McLean, G.S. Chandler, J. Chem. Phys. 72 (1980) 5639 (6-311G**).
[54] T. Clark, J. Chandrasekhar, P.v.R. Schleyer, J. Comp. Chem. 4 (1983) 294 (Diffuse functions).
[55] M.J. Frisch, J.A. Pople, J.S. Binkley, J. Chem. Phys. 80 (1984) 3265 (Multiple polarization functions).
[56] T.H. Dunning, P.J. Hay, in: H.F. Schaefer III (Ed.), Modern Theoretical Chemistry, vol. 3, Plenum Press, New York, 1976 (D95V basis set, p. 1).
[57] A. Wilson, van T. Mourik, T.H. Dunning, J. Mol. Struct. (Theochem) 388 (1997) 339 (and references cited therein, cc-pVnZ basis sets).
[58] M.J. Frisch, G.W. Trucks, H.B. Schlegel, P.M.W. Gill, B.G. Johnson, M.A. Robb, J.R. Cheeseman, T. Keith, G.A. Petersson, J.A. Montgomery, K. Raghavachari, M.A. Al-Laham, V.G. Zakrzewski, J.V. Ortiz, J.B. Foresman, J. Cioslowski, B.B. Stefanov, A. Nanayakkara, M. Challacombe, C.Y. Peng, P.Y. Ayala, W. Chen, M.W. Wong, J.L. Andres, E.S.Replogle, R. Gomperts, R.L. Martin, D.J. Fox, J.S. Binkley, D.J. Defrees, J. Baker, J.P. Stewart, M. Head-Gordon, C. Gonzalez, J.A. Pople, GAUSSIAN 94, Revision C.3; Gaussian Inc., Pittsburgh, PA, 1995.
[59] G. Herzberg, Electronic Spectra and Electronic Structure of Polyatomic Molecules, Molecular Spectra and Molecular Structure, vol. III, Van Nostrand Reinhold, New York,, 1966 (p. 599).
[60] A.D. Buckingham, R.L. Disch, D.A. Dunmur, J. Am. Chem. Soc. 90 (1968) 3104.
[61] C. Graham, D.A. Imrie, R.E. Raab, Mol. Phys. 1 (1998) 49.